Cohesin Smc1β determines meiotic chromatin axis loop organization

Ivana Novak,[1] Hong Wang,[1] Ekaterina Revenkova,[2] Rolf Jessberger,[2,3] Harry Scherthan,[4] and Christer Höög[1]

[1]Department of Cell and Molecular Biology, Karolinska Institutet, SE-171 77 Stockholm, Sweden
[2]Department of Gene and Cell Medicine, Mount Sinai School of Medicine, New York, NY 10029
[3]Institute of Physiological Chemistry, Dresden University of Technology, D-01307 Dresden, Germany
[4]Max Planck Institute for Molecular Genetics, D-14195 Berlin, Germany

Meiotic chromosomes consist of proteinaceous axial structures from which chromatin loops emerge. Although we know that loop density along the meiotic chromosome axis is conserved in organisms with different genome sizes, the basis for the regular spacing of chromatin loops and their organization is largely unknown. We use two mouse model systems in which the postreplicative meiotic chromosome axes in the mutant oocytes are either longer or shorter than in wild-type oocytes. We observe a strict correlation between chromosome axis extension and a general and reciprocal shortening of chromatin loop size. However, in oocytes with a shorter chromosome axis, only a subset of the chromatin loops is extended. We find that the changes in chromatin loop size observed in oocytes with shorter or longer chromosome axes depend on the structural maintenance of chromosomes 1β (Smc1β), a mammalian chromosome–associated meiosis-specific cohesin. Our results suggest that in addition to its role in sister chromatid cohesion, Smc1β determines meiotic chromatin loop organization.

Introduction

Meiosis is a specialized cell division process that is essential for haploid germ cell formation (von Wettstein et al., 1984; Zickler and Kleckner, 1999; Gerton and Hawley, 2005). After chromosome duplication at premeiotic S phase, the homologous chromosomes (each consisting of two sister chromatid pairs) acquire a structure made of two colinear proteinaceous axial structures from which chromatin loops emerge. Alignment of the homologous chromosomes (homologues) is initially promoted by a large number of DNA double-strand breaks at the leptotene stage of prophase I, which results in the formation of crossovers between the homologues. The homologues then become even more closely associated along their entire length through the addition of a large number of transverse filaments at the pachytene stage of prophase I (Heyting, 2005) in a process called synapsis. Ultrastructural analysis of meiotic cells at this stage reveals a distinct trilaminar structure called the synaptonemal complex (SC), which is composed of two axial/lateral elements surrounding a central element (von Wettstein et al., 1984; Zickler and Kleckner, 1999; Gerton and Hawley, 2005).

Correspondence to Christer Höög: christer.hoog@ki.se

H. Scherthan's present address is Institut für Radiobiologie der Bundeswehr, D-80937 Munich, Germany.

Abbreviations used in this paper: DKO, double knockout; SC, synaptonemal complex; SKO, single knockout; wt, wild type.

The online version of this article contains supplemental material.

The meiosis-specific protein Sycp3 has been shown to localize to the axial/lateral element regions of the SC and to give rise to filamentous structures when expressed in vivo (Lammers et al., 1994; Yuan et al., 1998), suggesting that the *Sycp3* gene encodes a component of the axial/lateral element. In agreement with this, inactivation of the *Sycp3* gene in mice results in loss of the axial/lateral element structures of the SC in meiotic cells (Yuan et al., 2000, 2002; Liebe et al., 2004). Importantly, analysis of *Sycp3*-deficient meiocytes has revealed a residual chromosome axis in the mutant cells that is twice as long as the chromosome axis seen in wild-type (wt) meiotic germ cells. This shows that the axial/lateral element contributes to axial compaction of the chromosomes but that this meiosis-specific structure is not essential for the formation of the chromosome axis (Yuan et al., 2000, 2002). *Sycp3*-deficient oocytes progress through meiosis I to the dictyate stage, and, after fertilization, a subset of those cells will give rise to viable offspring (Yuan et al., 2002).

What is the nature of the molecules that preserve the axial organization of the homologues in the absence of the axial/lateral elements? Additional axial structures that coexist with the axial/lateral element have been identified in some organisms using classic cytological methods or modified experimental staining/fixation methods (Dietrich et al., 1992; Zickler and Kleckner, 1999). Although the molecular nature of these axial structures is not known, molecules involved in forming the mitotic prophase

The Journal of Cell Biology, Vol. 180, No. 1, January 14, 2008 83–90
http://www.jcb.org/cgi/doi/10.1083/jcb.200706136

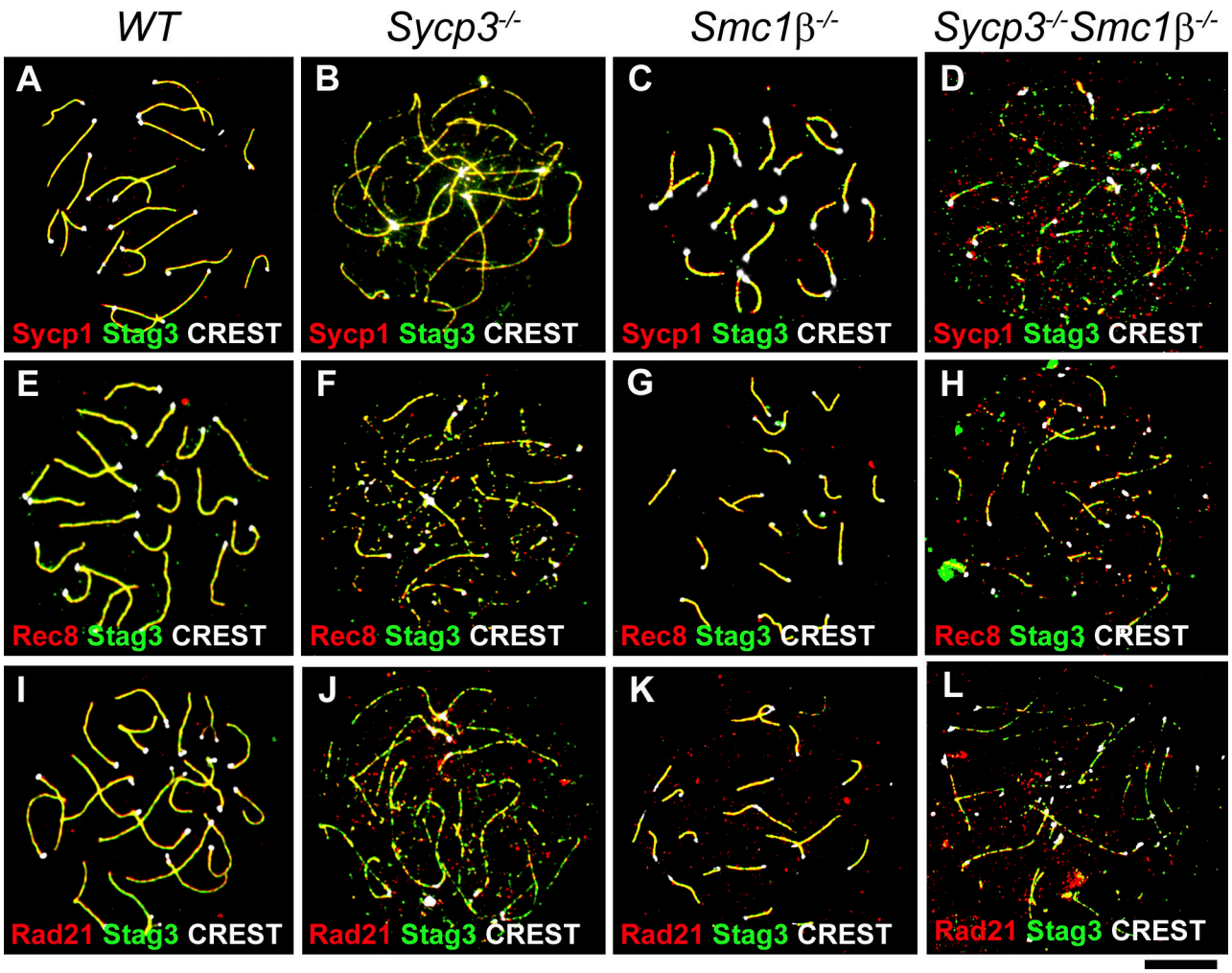

Figure 1. **Axial structures of the meiotic chromosomes formed by cohesin complexes in *Sycp3*$^{-/-}$*Smc1β*$^{-/-}$ oocytes remain but are fragmented.** Wt, *Sycp3*$^{-/-}$, *Smc1β*$^{-/-}$, and *Sycp3*$^{-/-}$*Smc1β*$^{-/-}$ pachytene oocytes (E18–18.5) were stained with antibodies against Sycp1 (red), Stag3 (green), and CREST (white; A–D); Rec8 (red), Stag3 (green), and CREST (white; E–H); and Rad21 (red), Stag3 (green), and CREST (white; I–L). Bar, 10 μm.

axes could also contribute to constructing a meiotic chromosome axis. Examples of these are topoisomerase II (Saitoh and Laemmli, 1994) and shape-determining architectural proteins (Strick and Laemmli, 1995). In addition, different cohesin complex proteins have been shown to colocalize with the residual axial structure seen in *Sycp3*-deficient meiotic cells (Pelttari et al., 2001).

The cohesin complex proteins mediate sister chromatid cohesion in mitotic and meiotic cells (Hirano, 2005; Nasmyth and Haering, 2005; Revenkova and Jessberger, 2005). The tetrameric cohesin complexes consist of two structural maintenance of chromosomes proteins, the heterodimeric Smc1 and Smc3, a kleisin protein such as Rad21 or Rec8, and a fourth subunit, an Sa/Stag protein. Prophase I meiocytes contain several types of cohesin complexes based on different combinations of two kleisin variants, two Smc1 variants, and three Sa protein variants. Of the two Smc1 variants, the ubiquitous Smc1α and the meiosis-specific Smc1β coexist on chromosome axes early in meiosis, but Smc1α disappears at the end of prophase I, and only Smc1β remains at centromeres until anaphase II (Eijpe et al., 2000; Revenkova et al., 2001, 2004). Interestingly, chromosomal axes shorten by ∼50% in *Smc1β*-deficient meiocytes compared with wt, which suggests a structural role for this protein in meiotic chromosome axis organization (Revenkova et al., 2004).

DNA recombination and chromosome segregation occur in synchrony with changes that affect chromatin organization during meiosis. Defects in chromatin organization are likely to have pronounced effects on the integrity of the genome; for example, Sycp3 inactivation results in impaired DNA repair, formation of achiasmatic chromosomes, and nondisjunction at the first meiotic division (Wang and Höög, 2006). One fascinating aspect of meiotic chromatin organization concerns the organization of the chromosome axis and the attached chromatin loops. Studies of human female meiotic chromosomes have shown that they are twofold longer than their male counterparts and that the chromatin loop is twofold shorter in oocytes compared with spermatocytes, suggesting an inverse relationship between axis length and chromatin loop size (Tease and Hulten, 2004; Kleckner, 2006). Therefore, the opposite changes in meiotic chromosome axis length seen in *Smc1β*- and *Sycp3*-deficient pachytene oocytes provide an opportunity to better understand the regulation of chromatin loop size and the attachment of loops to the axis. We have generated *Sycp3*$^{-/-}$*Smc1β*$^{-/-}$ double-knockout (DKO) mice to find out

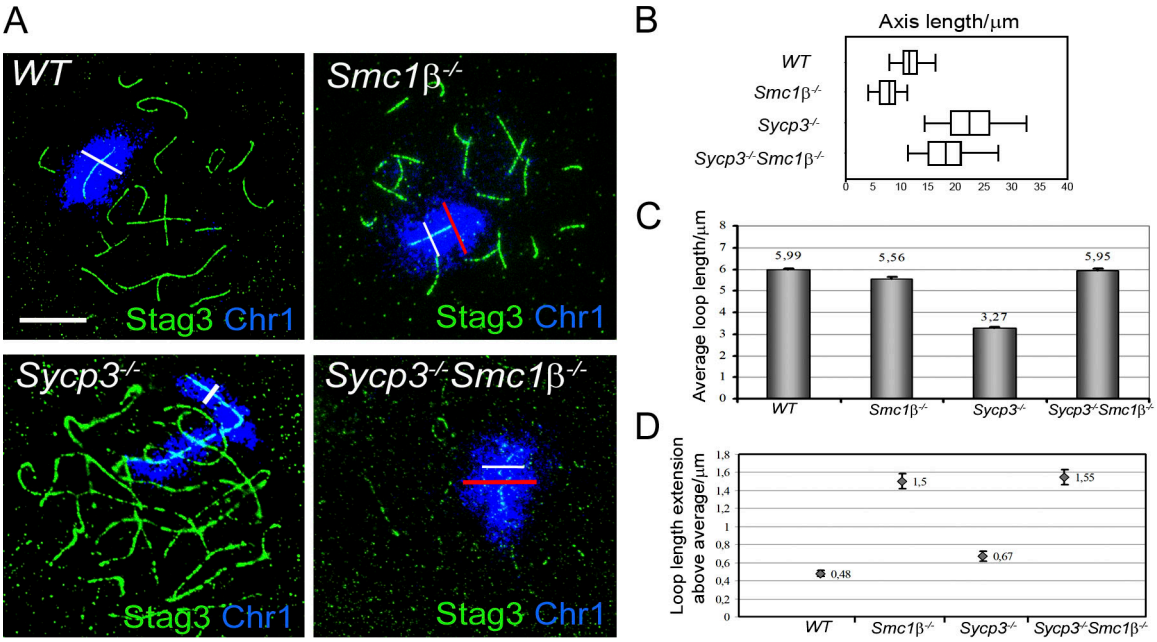

Figure 2. **Analysis of axial core and chromatin loop length.** Examples of the axial core and chromatin loop lengths in the four different genotypes. (A) White lines represent examples of mean loop length; red lines represent examples of maximum loop extensions. (B) Comparison of axial core length in wild-type (wt), *Sycp3*$^{-/-}$, *Smc1β*$^{-/-}$, and *Sycp3*$^{-/-}$*Smc1β*$^{-/-}$ oocytes after staining with Stag3 and a chromosome 1–specific probe. The mean axial core length was calculated from 70 wt and *Smc1β*$^{-/-}$oocytes and 50 *Sycp3*$^{-/-}$ and *Sycp3*$^{-/-}$*Smc1β*$^{-/-}$ oocytes. The statistical variability of the axial core lengths was visualized using a box plot method showing the median (the line in the center of the box) and the minimum and maximum values. (C) The mean length of the chromatin loops projecting from the sister chromatid axes was measured from one side of the FISH signal to the other (basal loops) in wt, *Sycp3*$^{-/-}$, *Smc1β*$^{-/-}$, and *Sycp3*$^{-/-}$*Smc1β*$^{-/-}$ oocytes. (D) Loop extensions were expressed as the differences between the maximum loop extension and mean chromatin loop length in wt, *Sycp3*$^{-/-}$, *Smc1β*$^{-/-}$, and *Sycp3*$^{-/-}$*Smc1β*$^{-/-}$ oocytes. (C and D) 50 oocytes from each genotype were analyzed, and the results are presented as mean ± SEM (error bars). Bar, 10 μm.

how the absence of both proteins affects chromosome axis length, chromatin loop size, and meiotic progression.

Results

Sycp3$^{2/2}$*Smc1b*$^{2/2}$ DKO pachytene oocytes retain a meiotic chromosome axis

We generated *Sycp3*$^{-/-}$*Smc1β*$^{-/-}$ DKO mice and analyzed them in parallel with *Sycp3*$^{-/-}$ and *Smc1β*$^{-/-}$ single-knockout (SKO) mice. We found that spermatocytes were eliminated at the early pachytene stage in DKO testes, resulting in a complete loss of male germ cells (unpublished data). In contrast, a loss of female germ cells in the two SKO mice strains is not observed until the dictyate stage of meiosis (Revenkova et al., 2004), so we used oocytes derived from wt, SKO, and DKO animals at embyonic day (E) 18–18.5 to study pachytene chromosome organization. The pachytene oocytes were stained with antibodies against the individual cohesin proteins Stag3, Rec8, or Rad21 (Fig. 1) or with an antibody against the transverse filament component of the SC, Sycp1. Importantly, extended meiotic chromosome axes, which were labeled by antibodies against the different cohesin complex proteins, remained in DKO oocytes (Fig. 1). These axes stained in a discontinuous pattern similar to that observed in *Sycp3*$^{-/-}$ oocytes.

We measured the chromosome axis length in four different genotypes using a combination of Stag3 staining of the axial structures and FISH painting of chromosome 1 (Fig. 2, A and B). In DKO pachytene oocytes, the mean axial core length was ∼18.3 μm, which is much longer than that seen in wt or *Smc1β*$^{-/-}$ oocytes but 20% shorter than observed in *Sycp3*$^{-/-}$ oocytes (Fig. 2 B).

Sycp3 absence in oocytes reduces chromatin loop size by 50%

Based on the impact of Sycp3 and Smc1β on chromosome axial length, we investigated whether chromatin loop size was affected in the SKO and DKO oocytes. We used the same combination of FISH (labeling mouse chromosome 1) and immunofluorescent staining using an anti-Stag3 antibody to monitor the distance that the chromatin extends from the chromosome axes (axis-distal extension/loop size). This distance was measured at a series of points along the chromosome 1 axes, and the mean distance was calculated (there was no statistically significant difference in values at specific points along the chromosome 1 axes). We found that the absence of Sycp3 in pachytene oocytes reduced the axis-distal extension of chromatin by almost 50% compared with wt cells (Fig. 2, A and C).

Simultaneous loss of Smc1β and Sycp3 restores chromatin loop size to wt levels

We then measured the mean axis-distal extension of the chromatin in *Smc1β*$^{-/-}$ pachytene oocytes and found it to be unaltered compared with wt (Fig. 2, A and C). However, in agreement with a previous study for *Smc1β*$^{-/-}$ spermatocytes (Revenkova et al., 2004), we found that a subset of loops along the chromosome axis projects much further from the axis than the mean

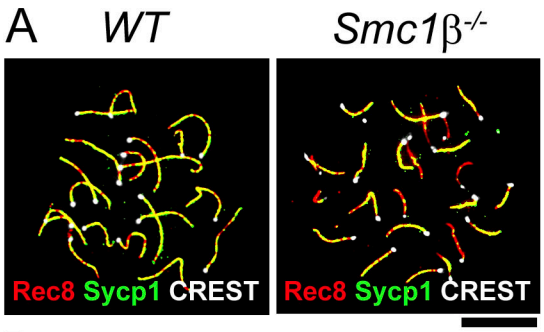

B

	Asynapsed chromosomes/number of cells analyzed				% of cells with asynapsed chromosomes
	Chr 19	Chr 17	Chr 12	Chr X	
Wt	0/208	0/208	0/156	0/156	**0**
Sycp3$^{-/-}$	7/196	3/196	0/111	2/111	**1.95**
Smc1β$^{-/-}$	23/160	11/160	10/189	21/189	**9.31**
Sycp3$^{-/-}$*Smc1β*$^{-/-}$	40/232	34/232	5/172	15/172	**11.63**

Figure 3. ***Smc1β*$^{-/-}$ and *Sycp3*$^{-/-}$*Smc1β*$^{-/-}$ oocytes show a high level of asynapsis at the pachytene stage.** (A) Staining of wild-type (wt) and *Smc1β*$^{-/-}$ pachytene oocytes (E18–18.5) with antibodies against Sycp1 (green), Rec8 (red), and CREST (white). Chromosomes labeled in yellow represent costaining of Sycp1 and Rec8, whereas chromosomes in *Smc1β*$^{-/-}$ pachytene oocytes with slight yellow staining represent asynapsed chromosomes. (B) Scoring of asynapsed chromosomes in wt, *Sycp3*$^{-/-}$, *Smc1β*$^{-/-}$, and *Sycp3*$^{-/-}$*Smc1β*$^{-/-}$ pachytene oocytes using FISH probes against chromosomes 12, 17, 19, and X. The percentage of asynaptic cells involving the four analyzed chromosomes (last column) was calculated as follows: the number of cells with asynapsis of one of the analyzed chromosomes was divided by the total number of cells analyzed for all four chromosomes, and the result was multiplied by 100. Bar, 10 μm.

approximation (Fig. 2 D). Importantly, the mean axis-distal chromatin extension was 5.9 μm in DKO, which is a twofold increase compared with *Sycp3*$^{-/-}$ oocytes, but was the same as observed in *Smc1β*$^{-/-}$ and wt oocytes (Fig. 2, A and C). Furthermore, as observed in the *Smc1β*$^{-/-}$ oocytes, the maximal distance of a subset of the chromatin loops in the DKO cells extended further (Fig. 2 D). In conclusion, we found that although chromatin loop size is reduced twofold in the absence of Sycp3, simultaneous inactivation of Smc1β restores the mean axis-distal chromatin projections in the DKO oocytes.

The axial structures represented by Sycp3 and Smc1β contribute to independent meiotic processes

Loss of Sycp3 or Smc1β has been shown to affect chromosome segregation in SKO mutant oocytes (Yuan et al., 2002; Revenkova et al., 2004; Hodges et al., 2005). Whereas the cause of the segregation defects in *Sycp3*-deficient oocytes has been linked to impaired DNA repair (Wang and Höög, 2006), no such link has been established in *Smc1β*-deficient oocytes. Alternatively, failure to complete synapsis could also cause segregation defects (Di Giacomo et al., 2005). Therefore, we initially determined whether synapsis was affected in *Smc1β*-deficient oocytes. Wt and *Smc1β*-deficient pachytene oocytes were stained with antibodies against Rec8, Sycp1, and with CREST (Fig. 3 A). We found that many of the *Smc1β*-deficient oocytes contained asynapsed chromosomes. Based on this result, pachytene oocytes from wt, the two SKO, and the DKO mice were subjected to chromosome painting by FISH to detect four different chromosomes (12, 17, 19, and X) and were combined with anti-Stag3 to identify the chromosome axes (Fig. 3 B). We found that an increased number of *Smc1β*$^{-/-}$ and DKO oocytes displayed asynapsis for all four analyzed chromosomes, whereas few *Sycp3*$^{-/-}$ oocytes and no wt oocytes contained such abnormal chromosomal configurations.

Asynapsis could contribute to incomplete crossing over and the formation of achiasmate chromosomes (univalents). Thus, the level of univalency in *Smc1β*$^{-/-}$ and DKO oocytes was evaluated at postnatal day 2 (that is, in dictyate-arrested oocytes). FISH analysis was used to score univalency levels affecting chromosome 17, chromosome 19, or both simultaneously in wt and mutant oocytes (Fig. 4, A and B). We found that univalency increased severely in *Smc1β*$^{-/-}$ oocytes in accordance with the elevated level of asynapsis detected in pachytene oocytes. Importantly, simultaneous inactivation of both Sycp3 and Smc1β substantially increased the percentage of oocytes that contained univalents (Fig. 4 B). The oocytes in the DKO animals are also lost at an accelerated rate compared with the two SKO genotypes, resulting in an almost complete elimination of oocytes by postnatal day 18 (Fig. 4 C and Fig. S1, available at http://www.jcb.org/cgi/content/full/jcb.200706136/DC1).

Discussion

Our results of the analysis of the *Sycp3*$^{-/-}$ and *Smc1β*$^{-/-}$ SKO mice and the *Sycp3*$^{-/-}$*Smc1β*$^{-/-}$ DKO mice are summarized in Table I. We find that *Smc1β*$^{-/-}$ oocytes have the same chromatin loop heterogeneity and level of asynapsis as DKO oocytes,

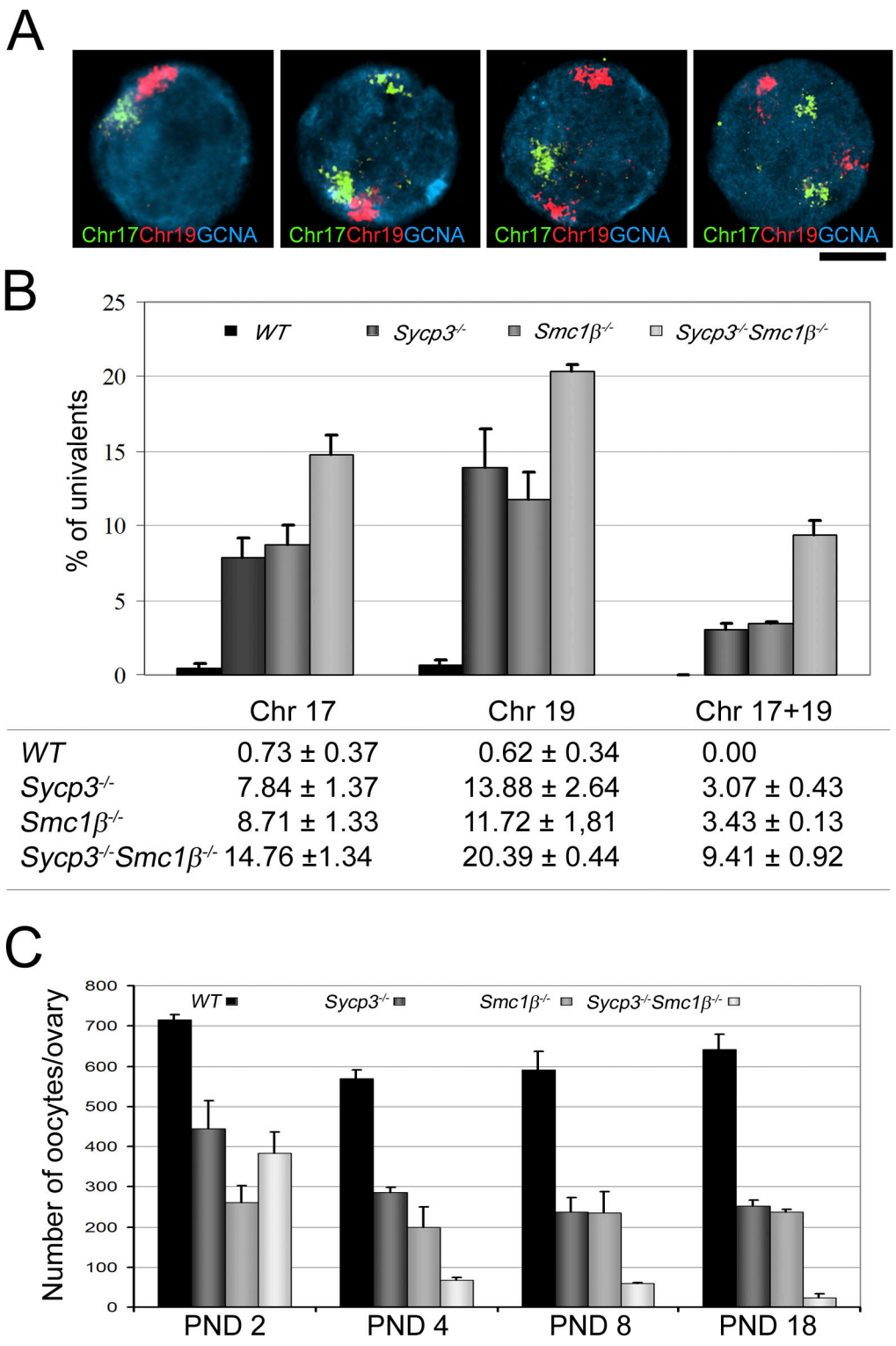

Figure 4. **Loss of both Sycp3 and Smc1β generates an additive increase in oocytes that contain univalent chromosomes.** (A) Examples of oocytes collected at postnatal day 2 with normal (far left) or univalent chromosomes 17, 19, or both. Oocytes were distinguished from ovarian somatic cells based on size and positive staining for germ cell nuclear antigen. (B) Percentage of univalency for chromosome 17, 19, or both in the four different genotypes as detected by FISH. The number of oocytes used to determine the percentages were 336 (wild type [wt]), 240 (*Sycp3*$^{-/-}$), 498 (*Smc1β*$^{-/-}$), and 303 (*Sycp3*$^{-/-}$*Smc1β*$^{-/-}$). Ovaries from three animals per genotype were used. (C) The number of oocytes per ovary in wt, *Sycp3*$^{-/-}$, *Smc1β*$^{-/-}$, and *Sycp3*$^{-/-}$ *Smc1β*$^{-/-}$ at days 2, 4, 8, and 18 after birth. A minimum of three ovaries per day and genotype were used. (B and C) The numbers are represented as mean ± SEM (error bars). PND, postnatal day. Bar, 10 μm.

Table I. **Summary of the results of the analysis of *Sycp3*$^{-/-}$, *Smc1β*$^{-/-}$, and *Sycp3*$^{-/-}$*Smc1β*$^{-/-}$ mice**

Phenotype	wt	*Smc1β*$^{2/2}$	*Sycp3*$^{2/2}$	*Sycp3*$^{2/2}$*Smc1β*$^{2/2}$	Comments
Cohesin staining	Continuous	Continuous	Gaps	Gaps	DKO = *Sypc3*$^{2/2}$
Core length (μm)	11.93	7.28	22.9	18.35	DKO not identical to any SKO
Loop length (mean)	Normal	Normal	Two times shorter	Normal	DKO = *Smc1β*$^{2/2}$
Loop length (extensions)	No	Yes	No	Yes	DKO = *Smc1β*$^{2/2}$
Asynapsis (%)	None	9.3	Rare	11.63	DKO = *Smc1β*$^{2/2}$
Univalents in dictyate (%)	0–0.7	3–12	3–14	9–20	DKO = *Sycp3*$^{2/2}$ + *Smc1β*$^{2/2}$
Oocyte loss	None	Some	Some	Faster	DKO = *Sycp3*$^{2/2}$ + *Smc1β*$^{2/2}$

showing that Smc1β acts before Sycp3 (i.e., is epistatic to Sycp3 in this context). We also find that axis integrity is affected similarly in *Sycp3*$^{-/-}$ and DKO oocytes, showing that Sycp3 is epistatic to Smc1β in maintaining longitudinal axis integrity. We found that axial core length and level of univalency in DKO oocytes differed from oocytes of both SKO genotypes. Thus, both genes contribute independently to the axial alterations and changes in univalency observed in the DKO oocytes.

Two distinct DNA checkpoints triggered by impaired DNA repair and asynapsis have been shown to monitor oocyte integrity and to promote elimination of damaged oocytes at the dictyate stage of meiosis (Di Giacomo et al., 2005). Our results show that Smc1β and Sycp3 contribute in an additive manner to the univalency level and the number of residual oocytes at the dictyate stage (hence the increased level of univalency and fewer oocytes seen in the DKO ovary). This could be explained by the independent activation of two DNA surveillance mechanisms in DKO oocytes: one triggered by the increased asynapsis observed in the *Smc1β*$^{-/-}$ oocytes (Fig. 3) and the other triggered by impaired DNA repair in *Sycp3*$^{-/-}$oocytes (Wang and Höög, 2006).

Smc1β and Sycp3 contribute to meiotic chromosome axis organization but are not required for its formation

One important outcome from this study is the identification of a basic chromosomal axial structure in DKO meiotic cells. We have previously shown that a residual chromosomal axis remains in *Sycp3*$^{-/-}$oocytes and that different cohesin complex proteins colocalize with this axis (Pelttari et al., 2001). Now, we show using the *Sycp3*$^{-/-}$*Smc1β*$^{-/-}$ DKO oocytes that Smc1β is not required for the formation of basic pachytene meiotic chromosome axes.

These results show that several layers of axis-associated proteins independently contribute to the formation and organization of the meiotic chromosome axes, possibly forming as a proposed supra-axial meshwork (Zickler and Kleckner, 1999). The nature of the molecules that give rise to the basic axes in meiotic cells is not known but could involve proteins that are also proposed to take part in mitotic chromosome axis formation such as topoisomerase II and shape-determining architectural proteins (Saitoh and Laemmli, 1994; Strick and Laemmli, 1995). Smc1β represents a second layer of proteins that colocalize with the axes but are not essential for its formation. This cohesin complex protein acts as a building block that contributes to axes length, as shown in *Smc1β*$^{-/-}$ oocytes (Revenkova et al., 2004) and in DKO oocytes, giving rise to an axis that was 20% shorter in the DKO oocytes than that seen in *Sycp3*-deficient oocytes (Fig. 2). Finally, Sycp3 represents a third layer of axis-associated proteins; in this case, as a component of an independent axial structure (the axial/lateral element) that coaligns with the meiotic chromosome axes and contributes to its longitudinal compaction.

Loss of Sycp3 reveals an inverse relationship between meiotic chromosome axis length and chromatin loop size

We have previously shown that Sycp3 is an essential component of the axial/lateral element of the SC and that the meiotic chromosome axis is twofold longer in *Sycp3*-deficient meiocytes (Yuan et al., 2000, 2002). We now show that the chromatin loops along the extended meiotic chromosome axis in *Sycp3*-deficient oocytes are twofold shorter than observed in wt oocytes. A reciprocal relationship has previously been postulated between axis length and chromatin loop extensions in meiotic cells (Zickler and Kleckner, 1999; Kleckner, 2006). This model suggests that the distance between individual loop attachment sites is conserved (i.e., a longer axis therefore means more loop modules in which, as a consequence, the individual loops become less extended). In agreement with this model, our results reveal a reciprocal relationship between increased axis length and reduced loop size, as determined by association of the axial/lateral element with the chromosome axis.

A role for Smc1β in chromatin loop organization

The localization of meiosis-specific cohesin complex proteins to the chromosome axes at prophase I aligns with their role in sister chromatid cohesion (Revenkova and Jessberger, 2005). However, we found that loss of Smc1β gave rise to loop heterogeneity in both SKO and DKO oocytes; that is, the maximal but not the mean loop extension was found to increase in *Smc1β*-deficient oocytes. Furthermore, the shortened chromatin loop size observed in oocytes lacking Sycp3 was restored to mean wt levels in DKO oocytes. The changes in chromatin loop size as a result of the presence or absence of Smc1β in the SKO and DKO oocytes are not easily reconciled with its role in cohesion or with changes in loop compaction. Early in structural maintenance of chromosomes protein research, however, it was suggested that cohesin complexes bound to the chromatin axes could act as chromatin loop attachment sites (Gasser, 1995; Hirano et al., 1995). Our results for Smc1β support a role for this cohesin complex protein in chromatin loop organization. We have

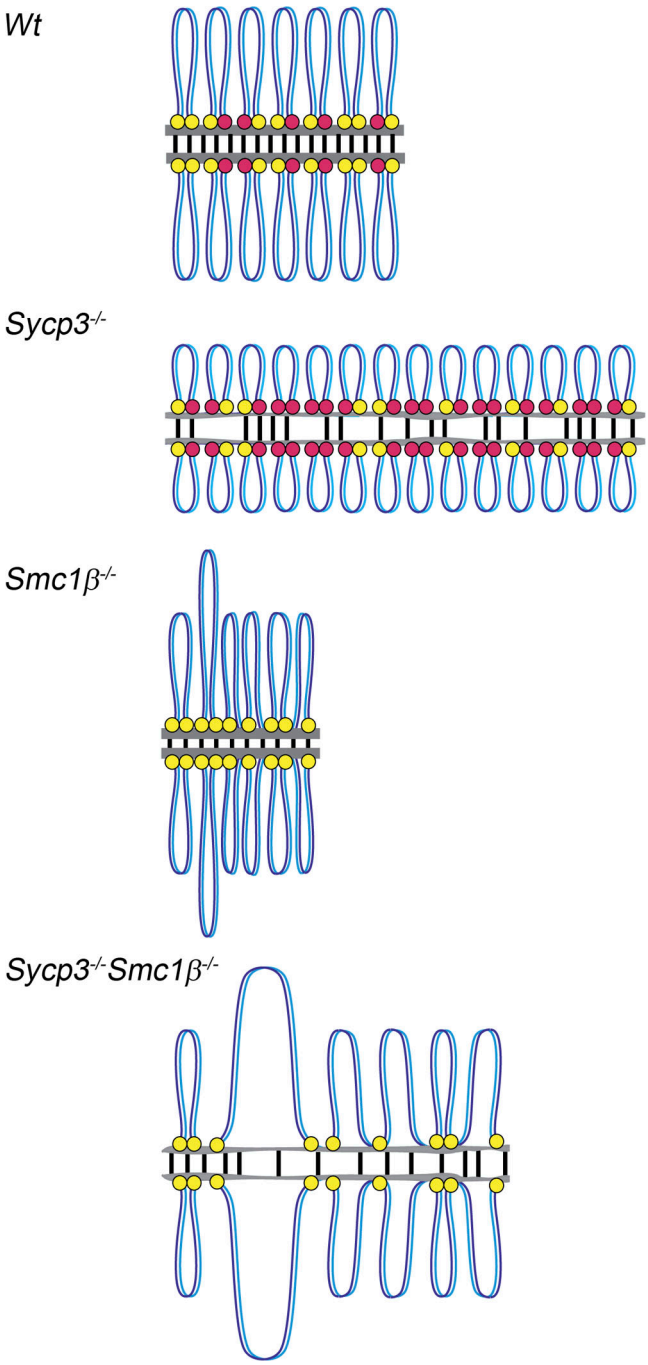

Figure 5. **Model of the effect of Sycp3 and two different cohesin complexes on both organization of the meiotic chromosome axes and chromatin loop extension.** Chromatin loops and axes are illustrated for wt, *Sycp3*$^{-/-}$, *Smc1β*$^{-/-}$, and *Sycp3*$^{-/-}$*Smc1β*$^{-/-}$ pachytene chromosomes. Lateral elements are shown as gray horizontal lines, and transverse filaments are shown as black vertical lines between each lateral element. Each loop contains the two sister chromatids. Red dots represent Smc1β-type cohesin complexes, and yellow dots represent Smc1α-type cohesin complexes. There are at least two types of cohesins, based either on Smc1β or on Smc1α. Several variants of each type may exist (not depicted). It is unclear whether the bases of the loops are determined by one cohesin complex or by several complexes together and/or whether these are of the same or different types. Thus, the model shows only one of several alternatives. The interpretation of the measured axis-distal chromatin projections assumes that chromatin is free to spread out equally well in wt and mutant oocytes (as supported by the loop heterogeneity observed in *Smc1β*-deficient oocytes and the variability in loop size observed in *Sycp3*-deficient and DKO oocytes).

summarized our experimental results in a model shown in Fig. 5. We suggest that in cells lacking Sycp3 (Sycp3 is first observed at the leptotene stage of prophase I, coinciding temporally with Smc1β expression), chromatin loop size is shortened as a result of the introduction of new, additional chromatin loops along the axis in response to axial extension. The alternative explanation that loss of Sycp3 affects loop compaction is unlikely, as this protein has not been reported to reside outside the axial/lateral element of the SC. Failure to retain the shortened chromatin loop size in the DKO oocytes suggests that the additional chromatin loops formed along the extended *Sycp3*$^{-/-}$ axis are determined by Smc1β. Our finding that the maximal but not the mean loop extension increased in *Smc1β*-deficient oocytes (that retain a functional axial/lateral element) further supports a role for Smc1β in loop organization.

Importantly, we do not observe a general extension of the axis-distal chromatin projections in the absence of Smc1β despite a shortening of the meiotic chromosome axis in this mutant. The variation from the expected reciprocal correlation between axes length and loop size (Zickler and Kleckner, 1999; Kleckner, 2006) in Smc1β-deficient oocytes may be explained by the presence of two Smc1 variants, α and β. The Smc1α-based somatic cohesin loads onto chromosomes as they replicate at the preleptotene stage of meiosis, thereby preceding expression and localization of Smc1β, which starts to appear during leptotene at the same time as Sycp3 (Eijpe et al., 2000; Revenkova et al., 2004). Therefore, it is likely that a large fraction of the chromatin loops is initially dependent on Smc1α but not Smc1β, which explains why only a subset of the loops is affected in Smc1β-deficient oocytes (Fig. 5). Our results suggest that the two Smc1 variants contribute independently to loop formation as meiosis progresses. The inability of Smc1α to substitute for Smc1β and to retain the shorter loops in *Smc1β*-deficient meiotic cells agrees with the decline in Smc1α expression during prophase I and the less uniform staining of the axes with anti-Smc1α antibodies (Eijpe et al., 2000; Revenkova et al., 2001).

Materials and methods

Mice

Derivation of the *Sycp3* and *Smc1β* knockout mice (both C57BL/6 strains) has been described previously (Yuan et al., 2000; Revenkova et al., 2004). *Sycp3* heterozygous mice were bred with *Smc1β* heterozygotes to generate double heterozygotes that were intercrossed to generate double *Sycp3*$^{2/2}$ *Smc1β*$^{2/2}$ mice. Experimental animals were compared with controls from the same litter (when possible) or from other litters from the same matings. Mice were genotyped by PCR as described previously using DNA from tail biopsies (Yuan et al., 2000). To detect pregnancy, females were caged with males, and the vaginal plugs were examined the following morning on a daily basis. The day that the plug was found was marked as embryonic day (E) 0.5. For ovary sampling at embryonic stages, pregnant female mice were killed at E16.5–18.5. To collect postnatally staged ovaries, the pups were killed from days 1–8 after birth (postnatal days 1–8).

Histology

Collected ovaries were fixed in 4% PFA for 4 h, paraffin embedded, and sectioned at 5 μm. To count the oocyte number in the ovaries, every fifth section was immunostained using antisera against germ cell–specific markers, either the germ cell nuclear antigen (Enders and May, 1994) or c-Kit (EMD). The number of oocytes in the ovaries derived from the different genotypes was calculated using histomorphometry methods as described by Wang and Höög (2006). Three to four ovaries per genotype were used for the analysis in each experimental group.

Immunofluorescence, the immuno-FISH procedure, and microscopy

Oocytes from embryonic or postnatal day 2 ovaries for immunostaining were prepared as described previously (Kouznetsova et al., 2005; Wang and Höög, 2006). In brief, ovaries were initially incubated with 400 U/ml collagenase in DME (Invitrogen) for 30 min at 37°C followed by 30 min in hypotonic buffer (30 mM Tris, pH 8.2, 50 mM sucrose, 17 mM sodium citrate, 5 mM EDTA, 0.5 mM DTT, and 0.5 mM PMSF). The cells were isolated by pipetting and were fixed with 1% PFA/0.15% Triton X-100. For protein detection and visualization, oocytes were stained with antibodies against Rec8, Stag3, Sycp1 (Kouznetsova et al., 2005), Rad21 (EMD), Smc3 (Eijpe et al., 2003), CREST, or germ cell nuclear antigen (Enders and May, 1994) followed by the secondary antibodies goat anti–mouse AlexaFluor488, goat anti–guinea pig AlexaFluor488 (Invitrogen), donkey anti–guinea pig CY3, goat anti–human CY5, mouse anti–rat FITC (The Jackson Laboratory), and swine anti–rabbit FITC (Dakopatts). If immunostaining was combined with FISH, the slides were first denatured in 70% deionized formamide/2× SSC at 70°C for 4 min and were hybridized with chromosome-specific probes (denaturation of the probe at 75°C for 10 min) for 40 h at 37°C. The single- and double-color chromosome probes were specific to chromosomes 1, 12, 17, or 19 and were directly labeled with CY3 or CY5 (Chrombios). Post-hybridization washing was performed according to the manufacturer's instructions. After FISH, slides were incubated with guinea pig anti-Stag3 (E18.5 oocytes) and visualized with goat anti–guinea pig AlexaFluor488 or mouse anti–rat FITC. Preparations were stained with DAPI and mounted in Prolong Antifade (Invitrogen). The preparations were viewed at room temperature using type F immersion liquid (n = 1.5180; Leica), microscopes (DMRXA2 and DMRXA; Leica), and a 100× NA 1.40–0.7 oil objective with epifluorescence or using an oil immersion objective (n = 1.515; Applied Precision), a DeltaVision Spectris system (Applied Precision), and a 60× NA 1.40 oil objective. The images were captured with a digital charge-coupled device camera (C4742-95; Hamamatsu) using Openlab software (Improvision) or were captured with a camera (1X-HLSH100; Olympus) using SoftWorx software (Applied Precision) and a microscope (DeltaVision; Applied Precision). Images were processed using Openlab, Photoshop CS2 (Adobe), or SoftWorx software. The core and loop length measurements were performed using SoftWorx, and statistical analysis was performed by one-way analysis of variance using SigmaStat (SPSS, Inc.).

Online supplemental material

Fig. S1 shows rapid elimination of the *Sycp3*$^{2/2}$*Smc1β*$^{2/2}$ oocytes. Online supplemental material is available at http://www.jcb.org/cgi/content/full/jcb.200706136/DC1.

We thank Dr. Nancy Kleckner for discussions of a previous version of this manuscript.

This work was supported by grants from the Swedish Cancer Society, the Swedish Research Council, and the Karolinska Institutet. H. Scherthan acknowledges support from H.H. Ropers (Max Planck Institute for Molecular Genetics, Berlin, Germany). R. Jessberger acknowledges support from the National Institutes of Health (grant GM R01 062517) and the Deutschen Forschungsgemeinschaft (grant JE 150/4-1/js).

Submitted: 20 June 2007
Accepted: 30 November 2007

References

Dietrich, A.J.J., J. van Marle, C. Heyting, and A.C. Vink. 1992. Ultrastructural evidence for a triple structure of the lateral element of the synaptonemal complex. *J. Struct. Biol.* 109:196–200.

Di Giacomo, M., M. Barchi, F. Baudat, W. Edelmann, S. Keeney, and M. Jasin. 2005. Distinct DNA-damage-dependent and –independent responses drive the loss of oocytes in recombination-defective mouse mutants. *Proc. Natl. Acad. Sci. USA.* 102:737–742.

Eijpe, M., C. Heyting, B. Gross, and R. Jessberger. 2000. Association of mammalian SMC1 and SMC3 proteins with meiotic chromosomes and synaptonemal complexes. *J. Cell Sci.* 113:673–682.

Eijpe, M., H. Offenberg, R. Jessberger, E. Revenkova, and C. Heyting. 2003. Meiotic cohesin REC8 marks the axial elements of rat synaptonemal complexes before cohesins SMC1β and SMC3. *J. Cell Biol.* 160:657–670.

Enders, G.C., and J.J. May II. 1994. Developmentally regulated expression of a mouse germ cell nuclear antigen examined from embryonic day 11 to adult in male and female mice. *Dev. Biol.* 163:331–340.

Gasser, S.M. 1995. Chromosome structure. Coiling up chromosomes. *Curr. Biol.* 5:357–360.

Gerton, J.L., and R.S. Hawley. 2005. Homologous chromosome interactions in meiosis: diversity amidst conservation. *Nat. Rev. Genet.* 6:477–487.

Heyting, C. 2005. Meiotic transverse filament proteins: essential for crossing over. *Transgenic Res.* 14:547–550.

Hirano, T. 2005. SMC proteins and chromosome mechanics: from bacteria to humans. *Philos. Trans. R. Soc. Lond. B Biol. Sci.* 360:507–514.

Hirano, T., T.J. Mitchison, and J.R. Swedlow. 1995. The SMC family: from chromosome condensation to dosage compensation. *Curr. Opin. Cell Biol.* 7:329–336.

Hodges, C.A., E. Revenkova, R. Jessberger, T.J. Hassold, and P.A. Hunt. 2005. SMC1beta-deficient female mice provide evidence that cohesins are a missing link in age-related nondisjunction. *Nat. Genet.* 37:1351–1355.

Kleckner, N. 2006. Chiasma formation: chromatin/axis interplay and the role(s) of the synaptonemal complex. *Chromosoma.* 115:175–194.

Kouznetsova, A., I. Novak, R. Jessberger, and C. Höög. 2005. SYCP2 and SYCP3 are required for cohesin core integrity at diplotene but not for centromere cohesion at the first meiotic division. *J. Cell Sci.* 118:2271–2278.

Lammers, J.H.M., H.H. Offenberg, M. van Aalderen, A.C.G. Vink, A.J.J. Dietrich, and C. Heyting. 1994. The gene encoding a major component of the lateral element of the synaptonemal complex of the rat is related to X-linked lymphocyte-regulated genes. *Mol. Cell. Biol.* 14:1137–1146.

Liebe, B., M. Alsheimer, C. Höög, R. Benavente, and H. Scherthan. 2004. Telomere condensation, meiotic chromosome condencation, pairing and bouquet stage duration are modified in spermatocytes lacking axial elements. *Mol. Biol. Cell.* 15:827–837.

Nasmyth, K., and C.H. Haering. 2005. The structure and function of SMC and kleisin complexes. *Annu. Rev. Biochem.* 74:595–648.

Pelttari, J., M.R. Hoja, L. Yuan, J.G. Liu, E. Brundell, P. Moens, S. Santucci-Darmanin, R. Jessberger, J.L. Barbero, C. Heyting, and C. Höög. 2001. A meiotic chromosomal core consisting of cohesin complex proteins recruits DNA recombination proteins and promotes synapsis in the absence of an axial element in mammalian meiotic cells. *Mol. Cell. Biol.* 21:5667–5677.

Revenkova, E., and R. Jessberger. 2005. Keeping sister chromatids together: cohesins in meiosis. *Reproduction.* 130:783–790.

Revenkova, E., M. Eijpe, C. Heyting, B. Gross, and R. Jessberger. 2001. Novel meiosis-specific isoform of mammalian SMC1. *Mol. Cell. Biol.* 21:6984–6998.

Revenkova, E., M. Eijpe, C. Heyting, C.A. Hodges, P.A. Hunt, B. Liebe, H. Scherthan, and R. Jessberger. 2004. Cohesin SMC1 beta is required for meiotic chromosome dynamics, sister chromatid cohesion and DNA recombination. *Nat. Cell Biol.* 6:555–562.

Saitoh, Y., and U.K. Laemmli. 1994. Metaphase chromosome structure: bands arise from a differential folding path of the highly AT-rich scaffold. *Cell.* 76:609–622.

Strick, R., and U.K. Laemmli. 1995. SARs are cis DNA elements of chromosome dynamics: synthesis of a SAR repressor protein. *Cell.* 83:1137–1148.

Tease, C., and M.A. Hulten. 2004. Inter-sex variation in synaptonemal complex lengths largely determine the different recombination rates in female and male germ cells. *Cytogenet. Genome Res.* 107:208–215.

von Wettstein, D., S.W. Rasmussen, and P.B. Holm. 1984. The synaptonemal complex in genetic segregation. *Annu. Rev. Genet.* 18:331–413.

Wang, H., and C. Höög. 2006. Structural damage to meiotic chromosomes impairs DNA recombination and checkpoint control in mammalian oocytes. *J. Cell Biol.* 173:485–495.

Yuan, L., J. Pelttari, E. Brundell, B. Björkroth, J. Zhao, J.G. Liu, H. Brismar, B. Daneholt, and C. Höög. 1998. The synaptonemal complex protein SCP3 can form multistranded, cross-striated fibers in vivo. *J. Cell Biol.* 142:331–339.

Yuan, L., J.G. Liu, J. Zhao, E. Brundell, B. Daneholt, and C. Höög. 2000. The murine SCP3 gene is required for synaptonemal complex assembly, chromosome synapsis, and male fertility. *Mol. Cell.* 5:73–83.

Yuan, L., J.G. Liu, M.R. Hoja, J. Wilbertz, K. Nordqvist, and C. Höög. 2002. Female germ cell aneuploidy and embryo death in mice lacking the meiosis-specific protein SCP3. *Science.* 296:1115–1118.

Zickler, D., and N. Kleckner. 1999. Meiotic chromosomes: integrating structure and function. *Annu. Rev. Genet.* 33:603–754.